Human Molecular Genetics, 2010, Vol. 19, No. 10 **2028–2038**
doi:10.1093/hmg/ddq084
Advance Access published on February 27, 2010

Identification and characterization of novel parathyroid-specific transcription factor *Glial Cells Missing Homolog B* (*GCMB*) mutations in eight families with autosomal recessive hypoparathyroidism

Michael R. Bowl[1,†], Samantha M. Mirczuk[1,†], Irina V. Grigorieva[1], Sian E. Piret[1], Treena Cranston[2], Lorraine Southam[3], Jeremy Allgrove[4,6], Shailini Bahl[5], Caroline Brain[6], John Loughlin[3,7], Zulf Mughal[8], Fiona Ryan[9], Nick Shaw[10], Yogini V. Thakker[11], Dov Tiosano[12], M. Andrew Nesbit[1] and Rajesh V. Thakker[1,*]

[1]Academic Endocrine Unit, Nuffield Department of Clinical Medicine, Oxford Centre for Diabetes, Endocrinology and Metabolism, University of Oxford, Churchill Hospital, Headington, Oxford OX3 7LJ, UK, [2]Oxford Medical Genetics Laboratories, Churchill Hospital, Headington, Oxford OX3 7LJ, UK, [3]Institute of Musculoskeletal Sciences, Botnar Research Centre, Nuffield Orthopaedic Centre, University of Oxford, Headington, Oxford OX3 7LD, UK, [4]Department of Paediatric Endocrinology, The Royal London Hospital, London E1 1BB, UK, [5]Childrens Unit, St Peter's Hospital, Chertsey, Surrey KT16 0PZ, UK, [6]Department of Endocrinology, Great Ormond Street Children's Hospital, Bloomsbury, London WC1N 3JH, UK, [7]Institute of Cellular Medicine, Musculoskeletal Research Group, Newcastle University, The Medical School, Framlington Place, Newcastle upon Tyne NE2 4HH, UK, [8]Department of Paediatrics, Saint Mary's Hospital for Women and Children, Manchester M13 OJH, UK, [9]Department of Paediatrics, The John Radcliffe Hospital, Headington, Oxford OX3 9DU, UK, [10]Department of Endocrinology, Birmingham Children's Hospital, Birmingham B4 6NH, UK, [11]Child Health Department, Milton Keynes Hospital, Milton Keynes MK6 5LD, UK and [12]Division of Endocrinology, Department of Pediatrics, Rambam Medical Center, Haifa 31096, Israel

Received December 10, 2009; Revised and Accepted February 20, 2010

GCMB is a member of the small transcription factor family GCM (glial cells missing), which are important regulators of development, present in vertebrates and some invertebrates. In man, *GCMB* encodes a 506 amino acid parathyroid gland-specific protein, mutations of which have been reported to cause both autosomal dominant and autosomal recessive hypoparathyroidism. We ascertained 18 affected individuals from 12 families with autosomal recessive hypoparathyroidism and have investigated them for *GCMB* abnormalities. Four different homozygous germline mutations were identified in eight families that originate from the Indian Subcontinent. These consisted of a novel nonsense mutation R39X; a missense mutation, R47L in two families; a novel missense mutation, R110W; and a novel frameshifting deletion, I298fsX307 in four families. Haplotype analysis, using polymorphic microsatellites from chromosome 6p23-24, revealed that R47L and I298fsX307 mutations arose either as ancient founders, or recurrent *de novo* mutations. Functional studies including: subcellular localization studies, EMSAs and luciferase-reporter assays, were undertaken and these demonstrated that: the R39X mutant failed to localize to the nucleus; the R47L and R110W mutants both lost DNA-binding ability; and the I298fsX307 mutant had reduced transactivational ability. In order to gain further insights, we undertook 3D-modeling of the GCMB DNA-binding domain, which revealed that the R110 residue is likely important for the structural integrity of helix 2, which forms part of

*To whom correspondence should be addressed. Tel: +44 1865857501; Fax: +44 1865857502; Email: rajesh.thakker@ndm.ox.ac.uk
†The authors wish it to be known that, in their opinion, the first two authors should be regarded as joint First Authors.

the GCMB/DNA binding interface. Thus, our results, which expand the spectrum of hypoparathyroidism-associated *GCMB* mutations, help elucidate the molecular mechanisms underlying DNA-binding and transactivation that are required for this parathyroid-specific transcription factor.

INTRODUCTION

Hypoparathyroidism (HPT) is an endocrine disorder in which hypocalcaemia and hyperphosphataemia are the results of a deficiency of parathyroid hormone (PTH) (1–3). Patients with HPT may develop seizures or tetany due to the hypocalcaemia. The inherited forms of HPT may occur as either isolated endocrinopathies with autosomal recessive, autosomal dominant or X-linked recessive transmission, or as part of complex congenital anomalies such as the DiGeorge (MIM #188400) and hypoparathyroidism-deafness-renal (HDR) dysplasia (MIM #146255) syndromes (http://www.ncbi.nlm.nih.gov/sites/entrez-?db=OMIM) (1,2,4–10). Autosomal dominant-HPT (AD-HPT) and autosomal recessive-HPT (AR-HPT) have been reported in association with germline mutations of the *PTH* gene (MIM *168450) (5–7), or the *Glial Cells Missing Homolog B* (*GCMB*) gene located on chromosome 6p24.2 (MIM *603716) (8,11–14). GCMB belongs to a small family of GCM transcription factors that are present in vertebrates and some invertebrates (15), which share a common zinc-coordinating DNA-binding domain (16), referred to as the GCM domain, that characteristically binds to a consensus motif 5′-ATGCGGGT-3′ (15,17,18). In mammals, there are two GCM proteins, referred to in man as GCMA and GCMB, and in mouse as Gcm1 and Gcm2. The N-terminal GCM domain of both proteins is evolutionarily highly conserved, but their C-terminal region, which contains two transactivation domains, is not conserved. The mammalian GCM proteins also differ in their temporal–spatial expressions (19–22). Gcm1 expression has been demonstrated in the foetal placenta, the late embryonic thymus and perinatally in the kidney (19,20), whereas Gcm2 expression appears to be restricted to the developing and adult parathyroid glands (21). Indeed, studies of a mouse deleted for Gcm2 have shown that Gcm2-deficient mice develop HPT, which can vary from severe hypocalcaemia causing early postnatal death, to mild hypocalcaemia that does not affect the viability or fertility of the mice (22). The HPT in these Gcm2-deficient mice has been shown to be due to a lack of parathyroid glands, thereby demonstrating the requirement of this parathyroid-specific transcription factor during murine parathyroid organogenesis (22).

To date, only three different homozygous GCMB mutations have been reported in patients with AR-HPT (Fig. 1) (8,11,12). These consist of a large intragenic deletion encompassing exons 1–4 and two missense mutations, R47L and G63S, which involved residues within the GCM DNA-binding domain (8,11–13). The R47L mutation abolished the normal DNA binding ability of the GCMB protein (12), while the G63S mutation did not alter DNA binding, but abolished the transactivation capacity of the GCMB protein (11). In order to understand further the mechanisms underlying this parathyroid developmental disorder and the role of the transcription factor, GCMB, we ascertained patients with AR-HPT and investigated them for *GCMB* mutations and their functional consequences.

RESULTS

GCMB genetic analysis in AR-HPT families

Eighteen individuals with AR-HPT from 12 families were ascertained (Table 1). In 11 families, the parents of the probands were known to be consanguineous. Ten families originated from the Indian Subcontinent, one family was from the Middle East and one family was from Somalia in Africa. DNA sequence analysis of the entire 1521 bp coding region, together with the associated splice sites and 5′ and 3′ untranslated regions of the *GCMB* gene, revealed the presence of 9 DNA sequence alterations in 9 of the 12 AR-HPT probands (Fig. 1 and Tables 1 and 2). Eight of these probands were homozygous for the DNA sequence alterations, consistent with an autosomal recessive trait, but one of the probands, from family 19/01, was heterozygous for the nucleotide substitution, and not consistent with an autosomal recessive association with the phenotype. This heterozygous substitution, which was located in exon 5 and resulted in a nonsynonymous change in the GCMB protein (Y282D), has been previously reported in an unrelated patient with HPT as a polymorphism, as it did not co-segregate with HPT in the family (23). This Y282D polymorphism was therefore not further investigated.

The eight homozygous GCMB mutations that were identified in eight of the AR-HPT probands consisted of four different mutations and these comprised a nonsense mutation (R39X), two missense mutations (R47L and R110W) and an intragenic deletion of 1 nucleotide that is predicted to result in a frameshift (fs) and a premature termination codon (I298fsX307) (Table 2 and Fig. 2). The I298fsX307 mutation was observed to occur in four AR-HPT families while the R47L mutant was observed in two AR-HPT families (Table 2 and Fig. 3). Haplotype analyses using three polymorphic microsatellite loci within a 4 Mbp region that flanked the *GCMB* locus on chromosome 6p24.2, was undertaken to assess for relatedness in these families that originated from the North-West region of the Indian Subcontinent. This revealed that among the four families with the I298fsX307 mutation (Fig. 2), two families (1/04 and 11/08) were likely to have had a common ancestor, but that the other two families (9/06 and 1/05) are unrelated (Fig. 3). Furthermore, analysis of family 1/05, in which the parents are non-consanguineous, revealed that the I298fsX307 mutation had arisen independently in the father and mother (Fig. 3). These results, which show the repeated occurrence of the I298fsX307 mutation on different haplotypes, indicated that this may be a potential mutational ‘hot-spot’. A similar analysis of the two families (11/07 and 16/08) harbouring the R47L mutation

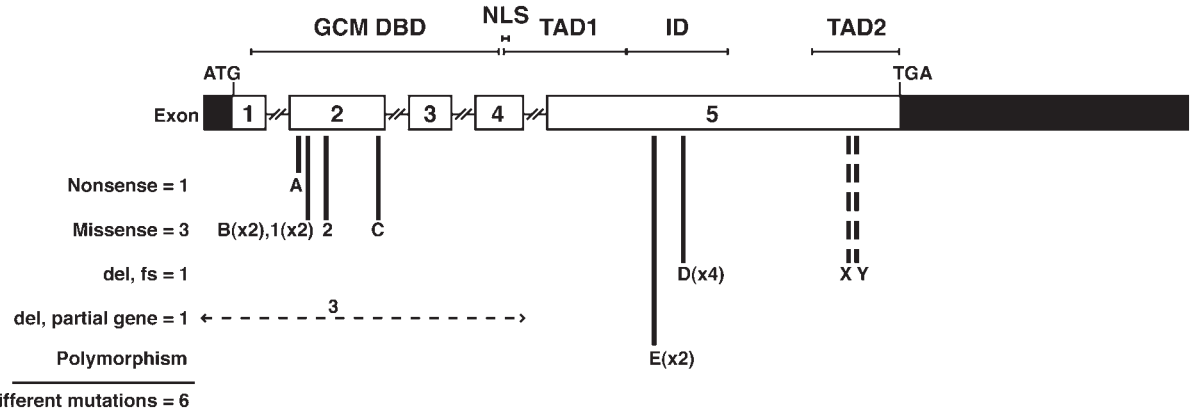

Figure 1. Schematic representation of the genomic structure of the *GCMB* gene illustrating the locations of mutations identified in AR-HPT patients. The human *GCMB* gene consists of five exons, spanning ~15 Kb of genomic DNA on chromosome 6p24.2 and encodes a 506 amino acid transcription factor that contains a GCM DNA-binding domain (*GCM DBD*), two transactivation domains (*TAD1* and *TAD2*), an inhibitory domain (*ID*) and a predicted nuclear localization signal (NLS) at residues 176–191 (24). The sizes of exons 1, 2, 3, 4 and 5 are 162, 253, 113, 126 and 1703 bp, respectively. The ATG (translation start) and the TGA (Stop) sites are in exons 1 and 5, respectively, and the untranslated regions (5′ and 3′) are shown in black. The locations of the four homozygous *GCMB* mutations (letters A to D), together with one heterozygous polymorphisms (Y282D, letter E), identified in nine AR-HPT probands by the present study are shown. The details of these DNA sequence alterations are shown in Table 2. In addition, the three previously reported homozygous mutations R47L, G63S and deletion involving exons 1–4, are shown numbered 1 to 3, respectively (8,11–13). The polymorphism Y282D (letter E) has been previously reported in an unrelated patient (23). Mutation D was found to occur in four probands, and mutation B, which has been previously reported in two probands (mutation 1) (12,13), was found to occur in a further two probands. This yields a total of six different homozygous *GCMB* abnormalities in 12 AR-HPT patients. In addition, the two previously reported heterozygous AD-HPT-causing *GCMB* mutations c.1389delT and c.1399delC are shown labelled X and Y, respectively (13,14).

Table 1. Clinical and serum biochemistry findings in 18 AR-HPT patients in 12 families

Mutation/ polymorphism[a]	Family/patient (sex[b])	Hypoparathyroidism Serum Ca^{2+} mmol/l[c]	Serum PTH (assay range)[d]	Presentation[e]	Age[f]	Geographical origin[g]
A	1/07 Proband (M)	1.29	UD	I	14 days	In
B	11/07 Proband (F)	0.90	3 pg/ml (10–65)	Se	9 days	In
	Brother (M)	1.36	<10 pg/ml	Se	5 days	In
B	16/08 Proband (F)	1.35	<10 pg/ml (10–50)	Se	6 weeks	In
	Sister (F)	2.02	<10 pg/ml	As	1 week	In
C	13/08 Proband (M)	1.10	<0.3 (1–6)	Se	1 year	In
	Mother (F)	1.36	N/D	Se	25 years	In
D	9/06 Proband (M)	1.17	<1 pg/ml (7–53)	Se	4 weeks	In
D	1/04 Proband (F)	1.51	UD	Te/Se	2 weeks	In
	Brother (M)	1.13	UD	Te/Se	<4 weeks	In
D	1/05 Proband (F)[h]	1.25	UD	Se	9 days	In
D	11/08 Proband (F)	1.74	<6 pg/ml (11–65)	Se	4 months	In
E	19/01 Proband (M)	1.35	6.5 pg/ml (12–70)	Te	8 years	Me
Nd[i]	1/06 Proband (M)	1.26	<5 pg/ml (10–60)	Se	3 years	Sa
	Sister (F)	1.28	7 pg/ml (10–60)	I/Te	9 years	Sa
Nd[i]	1/03 Proband (M)	1.02	8.3 ng/l (10–29)	Se	4 weeks	In
	Brother (M)	1.57	6 ng/l (10–29)	Se	15 months	In
Nd[i]	2/89 Proband (M)	1.71	<16 ng/l (20–80)	P	3 weeks	In

[a]Mutation/polymorphism, location and details are shown in Figure 1 and Table 2, respectively.
[b]Sex: M, male; F, female.
[c]L: low, exact value not known, serum total calcium-pretreatment values (normal range = 2.10–2.60). N/A denotes details not available.
[d]Serum PTH: UD, undetectable; N/D, not determined.
[e]As, asymptomatic; I, irritability; Se, seizures; Te, tetany; P, poor feeding and weight gain.
[f]Age at diagnosis.
[g]In, Indian Subcontinent; Me, Middle East; Sa, Somalia (Africa).
[h]Non-sanguineous family. All other families were consanguineous.
[i]Nd, None detected.

revealed that the families were unrelated and that the mutation had arisen independently within a potential 'hot-spot'. Three of these mutations, the R39X, R110W and I298fsX307, have not been previously reported, while the R47L has been reported in two other families (12,13). The occurrences of the mutations were confirmed by restriction endonuclease analysis (Fig. 2 and Table 2), and individuals affected with AR-HPT were demonstrated to be homozygous while their unaffected normocalcaemic parents and siblings were heterozygous, consistent with an autosomal recessive disorder (Fig. 2). The absence of all of these DNA sequence abnormalities in 110 alleles from 55 unrelated normal individuals

Table 2. GCMB DNA sequence alterations detected in nine AR-HPT patients

Mutation/polymorphism[a]	Family[b]	Exon	Codon	Base change	AA change	RE[c]	Effect[d]
Nonsense mutation							
A	1/07	2	39	**C**GA → **T**GA	Arg → Stop	*Dde*I	Loss of DBD, TAD 1&2, NLS, and ID
Missense mutation							
B	11/07	2	47	C**G**C → C**T**C	Arg → Leu	*BsaHKA*I	Disruption of DBD
B	16/08	2	47	C**G**C → C**T**C	Arg → Leu	*BsaHKA*I	Disruption of DBD
C	13/08	2	110	**C**GG → **T**GG	Arg → Trp	*Nla*III	Disruption of DBD
Intragenic deletion							
D	1/04	5	298	ATC → A–C	Frameshift	*Rsa*I	Premature termination[e]
D	1/05	5	298	ATC → A–C	Frameshift	*Rsa*I	Premature termination[e]
D	9/06	5	298	ATC → A–C	Frameshift	*Rsa*I	Premature termination[e]
D	11/08	5	298	ATC → A–C	Frameshift	*Rsa*I	Premature termination[e]
Polymorphism							
E	19/01	5	282	**T**AT → **G**AT	Tyr → Asp	*Hph*I	None[f]

[a]Mutation/polymorphism letter refers to location shown in Figure 1.
[b]Family identification refers to clinical details shown in Table 1.
[c]Mutation/polymorphism confirmed using analysis by restriction endonuclease (RE) digestion.
[d]DNA-binding domain (DBD); transactivation domain (TA); nuclear localization signal (NLS); inhibitory domain (ID).
[e]Missense peptide 9 amino acids from 298 to 306, followed by premature stop at codon 307; truncated protein with disruption of the ID and loss of TAD2.
[f]Likely no functional effect, as previously reported to not co-segregate with HPT (23).

indicated that these DNA sequence changes were mutations and not functionally neutral polymorphisms that would be expected to occur in >1% of the population.

The R47L mutation has been previously reported to lead to disruption of DNA binding activity, and the three newly identified mutations (R39X, R110W and I298fsX307), which occurred in exons 2 or 5 (Fig. 1), predict structurally significant changes (Table 2). Thus, the R39X mutation is predicted, if translated, to lead to a truncated GCMB protein lacking the DNA-binding domain (DBD), the predicted nuclear localization signal (NLS) and both transactivation domains (TAD1 and 2); the R110W mutation involves substitution of a highly conserved, basic, hydrophilic arginine for an aromatic, hydrophobic tryptophan residue within the DBD, and is predicted to disrupt the correct folding of this protein domain and hence affect its ability to bind DNA; and the frameshift deletion I298fsX307 is predicted to lead to a loss of the C-terminal 209 amino acids of GCMB (298 to 506), and hence a loss of the C-terminal TAD2 (Table 2) that would lead to a reduction in transactivational ability. GCM mutations were not detected in ~33% (4 of the 12) of the AR-HPT families, although our study did not search for intronic mutations. A comparison of the phenotypes in patients harbouring GCMB mutations with those without GCMB mutations revealed no significant differences (Table 1), suggesting that it would be difficult to predict the likelihood of a *GCMB* mutation being the underlying cause on the basis of clinical findings. The functional effects of these four different identified *GCMB* mutations (Table 2 and Fig. 1) were assessed further.

Nuclear localization studies

To assess the functional significance of the mutations on GCMB (Table 2 and Fig. 1) which is known to contain a predicted NLS at residues 174 to 191 (24), we transfected COS-7 cells with green fluorescent protein (GFP)-tagged wild-type and mutant GCMB constructs. Fluorescence microscopy revealed that the wild-type GCMB protein and three of the mutant (R47L, R110W and I298fsX307) GCMB proteins that retain the predicted NLS were exclusively localized to the nucleus. However, the R39X mutant, which lacks the predicted NLS, did not accumulate in the nucleus and resembled the result found for GFP vector alone (Fig. 4), consistent with a loss of nuclear localization. These results indicate that the three mutants (R47L, R110W and I298fsX307) which localize to the nucleus may alter the transactivating capacity of GCMB, whereas the R39X mutant that lacks the DBD, NLS and TAD1 and (Fig. 1 and Table 2) two domains and does not localize exclusively to the nucleus is unlikely to influence transactivation function. The three GCMB mutants, R47L, R110W and I298fsX307, were therefore further investigated for DNA-binding and transactivation activity.

DNA binding studies

The R47L, R110W and I298fsX307 GCMB mutants did not affect the nuclear localization, and we therefore performed electrophoretic-mobility shift assays (EMSAs) using nuclear extracts from COS-7 cells transfected with wild-type or mutant GCMB c-Myc tagged constructs to investigate the DNA binding properties of the wild-type and mutant GCMB proteins (Fig. 5). The GCMB mutant I298fs307X retained DNA-binding, whereas the two GCMB missense mutants R47L and R110W, which involve highly conserved residues (Fig. 6) within the GCM DBD (residues 19–174) (Fig. 1 and Table 2), failed to bind the DNA consensus recognition motif (Fig. 5). To elucidate further the structural requirements of the R47 and R110 residues for DNA-binding we undertook comparative modelling studies of the GCMB–DNA complex.

Three-dimensional modelling the GCMB–DNA complex and the predicted effects of the GCMB mutants R47L and R110W

The GCM family of proteins share a structurally common DBD, and alignment of the mouse Gcm1 DBD (residues 14–171) with that of the human GCMB (residues 19–176) demonstrated a 68% identity between the two domains

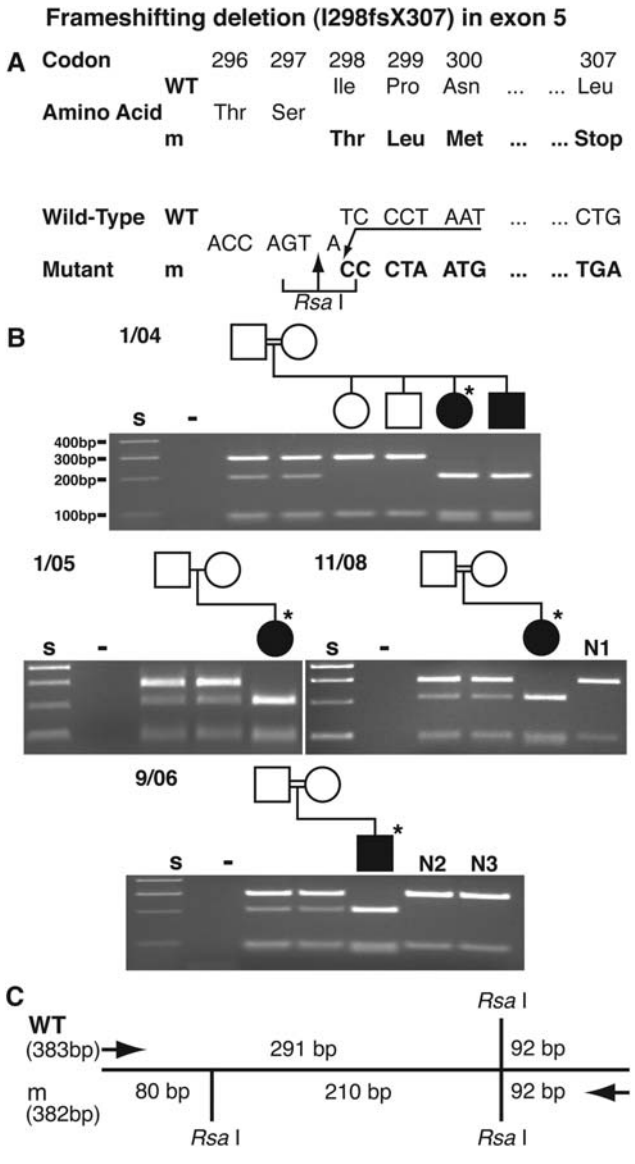

Figure 2. Detection of a *GCMB* frameshifting-deletion mutation in exon 5 in four families with AR-HPT by restriction enzyme analysis. (**A**) DNA sequence analysis of each proband revealed a 1 bp deletion (nucleotide 893) at codon 298, thus altering the wild-type (WT) sequence ATC, encoding an isoleucine (Ile, I), to the mutant (m) sequence A**CC**, encoding a threonine (Thr, T). This single base deletion is predicted to lead to a frameshift with the incorporation of nine missense amino acids followed by a premature termination signal at codon 307. The frameshift deletion also resulted in the gain of an *Rsa* I restriction endonuclease recognition motif (GT/AC). (**B**) *Rsa* I restriction endonuclease analysis facilitated the confirmation of the mutation in the families (probands are denoted by an asterisk). (**C**) PCR amplification and *Rsa* I digestion would result in two products of 291 and 92 bp from the wild-type (WT) allele, but three products of 210, 92 and 80 bp from the mutant (m) allele, as illustrated in the restriction map. All the five individuals affected with HPT are homozygous, whereas their asymptomatic, normocalcaemic parents are heterozygous, consistent with an autosomal recessive inheritance of this disorder. The parents in families 11/04, 11/08 and 9/06 were known to be consanguineous, whereas the parents from family 1/05, who were heterozygous for the mutation, were not known to be consanguineous and this was confirmed by haplotype analysis (Fig. 3). Absence of this frameshifting deletion in 110 alleles from 55 unrelated normal individuals (N1 to N3 shown) indicates that it is not a common DNA sequence polymorphism. Individuals are represented as male (square); female (circle); unaffected (open symbol); affected (filled symbol); S, DNA size markers from a 100 bp ladder; -, no DNA control.

(Fig. 6A). This level of homology allowed a reliable model of the GCMB DBD in complex with DNA to be determined by comparative modelling, based on the previously published Gcm1-DNA crystal structure (PDB ID: 1ODHA, http://www.ebi.ac.uk/pdbe/) (25) (Fig. 6B). This model was used to study the structural consequences that may explain the disruption of DNA-binding by the R47L and R110W mutants. The AR-HPT associated GCMB R47L mutation is not located on the DNA-binding interface of GCMB, thereby suggesting that this mutation affects DNA binding through an indirect mechanism (12,25). More recently, using modelling of the GCMB–DNA complex at an atomic structural level, it has been shown that R47 forms a side-chain hydrogen bond with D22, which cannot form in the L47 mutant, and that this interaction is important for stabilizing the amino-terminal region of GCMB (Fig. 6C) (26). Thus, loss of this polar side-chain interaction in the R47L mutant is likely to lead to misfolding or destabilization of the GCMB protein. A similar analysis of the AR-HPT associated GCMB R110W mutation, which is located within a helix that forms part of the DNA-binding interface, predicts that three side-chain hydrogen bonds form between R110 and the highly evolutionarily conserved residues A104, I105 and D107 (Fig. 6D and E). These three hydrogen bonds are likely required, in the wild-type protein, for the stabilization of the strand-bend-helix structure that fits into the DNA groove (Fig. 6D). However, the W110 mutation predicts a loss of formation of these potentially stabilizing polar contacts as the substitution of the aromatic tryptophan residue at this position, which has a larger van der Waals volume compared with arginine, may sterically hinder the correct folding of the GCMB protein, and thereby disrupt the DNA binding interface with a consequent loss of DNA-binding by the mutant GCMB protein.

Luciferase reporter assays

The effects of the AR-HPT GCMB mutants on gene expression were assessed by luciferase reporter assays (Fig. 7), in which wild-type and mutant GCMB c-Myc tagged constructs were co-transfected into DF-1 cells, with a CaSR-promoter (P1) luciferase reporter vector, which has recently been shown to contain a responsive endogenous GCMB DNA recognition site (13). Co-expression of the P1 construct with wild-type GCMB resulted in a significant increase, by ~2-fold increase in relative luciferase activity, when compared with that of the empty pCMV-Myc vector. Expression of each of the mutant GCMB (R47L, R110W or I298fsX307) constructs alone with the P1 construct did not increase relative luciferase activity when compared with that of empty vector, thus indicating loss of transactivational capacity of these mutant GCMB proteins (Fig. 7). However, co-transfection of the mutant GCMB R47L or R110W constructs with the wild-type GCMB construct had no effect on the transcription activity which was similar to that of the wild-type alone (Fig. 7). These results are consistent with the autosomal recessive inheritance of these GCMB mutations. However, co-transfection of the mutant GCMB I298fsX307 construct with the wild-type GCMB construct resulted in only a ~1.1-fold increase in transcriptional activity when compared with that of the empty vector (Fig. 7). The I298fsX307, which can bind DNA (Fig. 5) and has an intact

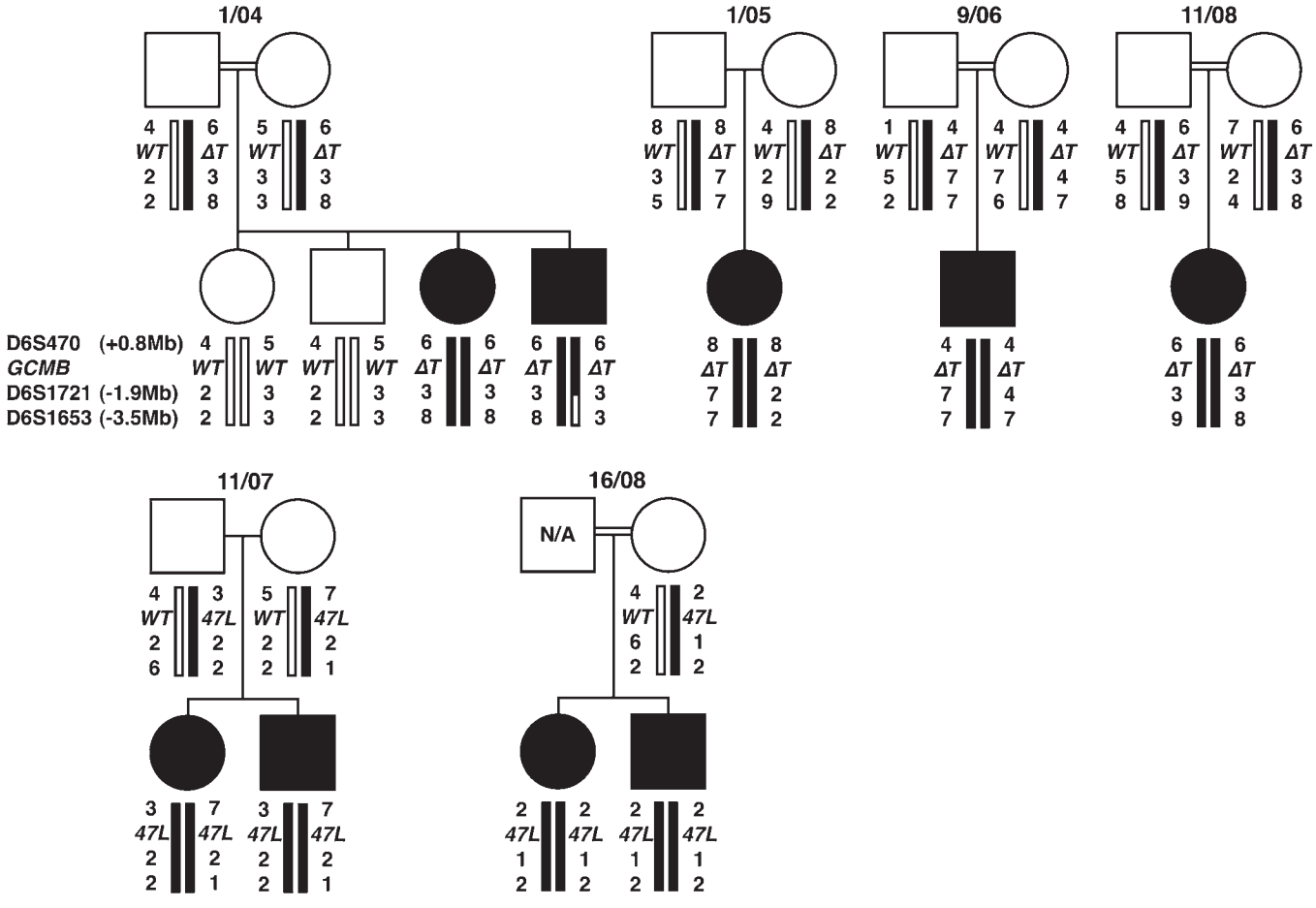

Figure 3. Haplotype analysis using chromosome 6p23-24 loci and the *GCMB* mutation in AR-HPT families. The genotypes at the 3 chromosome 6p23-24 microsatellite polymorphic loci 6pter-D6S470-D6S1721-D6S1653-6pcen that span an approximate 4 Mb region were ascertained in the four families with the *GCMB* frameshifting deletion (I298fsX307) in exon 5 (Fig. 2) and the 2 families with the R47L mutation (Table 2). The GCMB locus is flanked by D6S470 and D6S1721 and the size of the respective intervals are indicated in parenthesis. The paternal haplotypes are on the left and the maternal haplotypes are on the right. Analysis of the four families (1/04, 1/05, 9/06 and 11/08) harbouring the I298fsX307 mutation demonstrated inheritance of a single mutant allele within each of the three families (1/04, 9/06 and 11/08) consistent with consanguinity. In addition, the haplotypes carrying the *GCMB* mutation in families 1/04 and 11/08 are identical, thereby suggesting relatedness. Analysis of family 1/05 demonstrated that the two parental mutant allele haplotypes differed at 2 of the 3 loci, thereby indicating that this mutation had likely arisen independently in the ancestors of the father and mother. Analysis of the two families (11/07 and 16/08) harbouring the R47L mutation demonstrated inheritance of a single mutant allele in family 16/08, consistent with consanguinity. However, in family 1/05 the two parental haplotypes harbouring the *GCMB* mutation differed at 2 of the 3 loci, thereby indicating that the parents are non-consanguineous and that this R47L mutation had arisen independently in the ancestors of the father and mother. The symbols denoting individuals are as described in Figure 2. N/A, not available.

TAD1 (Fig. 1), only resulted in AR-HPT in homozygous individuals but not in heterozygous individuals (Fig. 2), indicating that the mildly decreased level of ~1.1-fold activity may still be above a threshold value needed to fulfil the cellular function of GCMB as a transcription factor in heterozygous individuals. This would be consistent with the findings of other transcription factors for which such dosage effects, which are above a critical level and able to promote organ development, have been reported (27).

DISCUSSION

Our results, which have identified four different mutations of the *GCMB* gene (Table 2) in eight probands and their families, expand the spectrum of mutations, report the first nonsense and frame-shifting deletion mutations, and further establish the role of GCMB in the aetiology of this developmental disorder. In addition, our studies of these *GCMB* mutations help increase our understanding of the underlying DNA binding and transactivation that are involved in the function of this parathyroid gland-specific transcription factor. Thus, the four mutations (R39X, R47L, R110W and I298fsX307) identified in *GCMB* which cause AR-HPT lead to reduced transactivation by one of three mechanisms: mislocalization (R39X), loss of DNA binding (R47L and R110W) or loss of transactivation (I298fsX307). Finally, our findings show that the I298fsX307 and R47L mutations have arisen independently in unrelated AR-HPT families from the North-West region of the Indian Subcontinent. Such recurrent mutations have been called mutation 'hotspots' (28), and these may be associated with nucleotide substitutions or deletions within homonucleotide repeats, or during the repair of mismatches caused by heteroduplex formation between imperfect direct repeats (29–32). However, neither of these recurrent mutations, R47L and

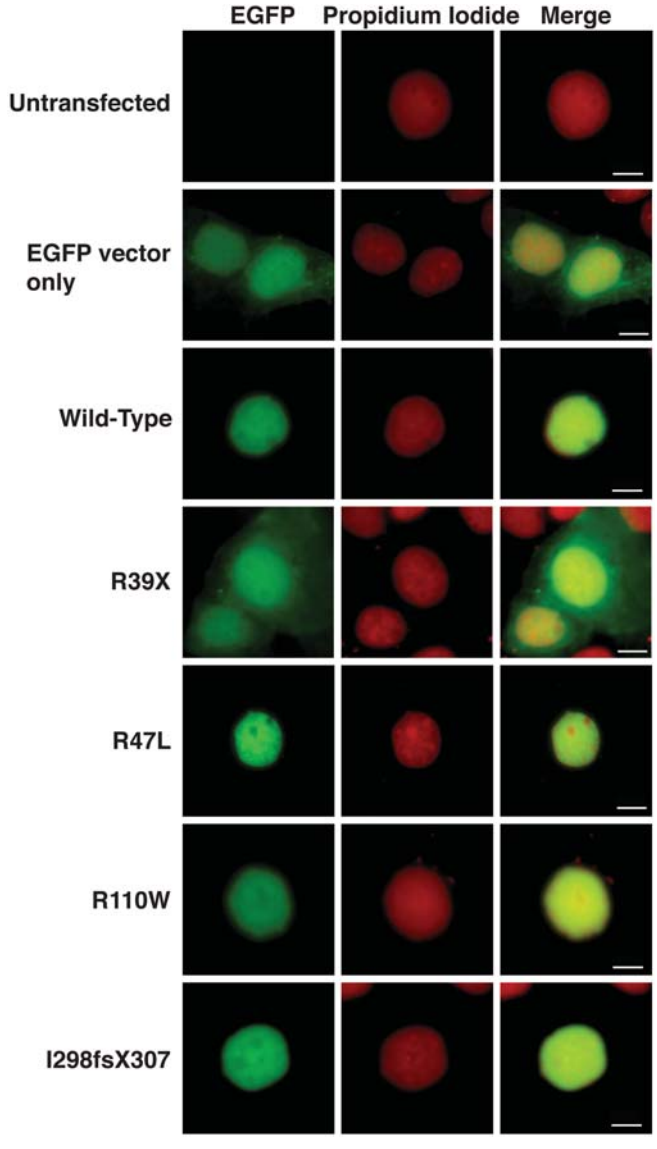

Figure 4. Subcellular localization of wild-type and GCMB mutants identified in patients with AR-HPT. COS-7 cells were transfected with either EGFP–GCMB constructs or empty EGFP-vector. COS-7 cells that were transfected with EGFP alone or that were untransfected were used as controls. At 24 h post-transfection, cells were fixed and stained using propidium iodide to identify nuclei. Fluorescence microscopy, using the appropriate filters, was performed to detect EGFP (green) and propidium iodide (red) signals. Nuclear localization was confirmed by merging the images and detection of yellow emission. The wild-type GCMB localized to the nucleus. In addition, the three GCMB mutants, R47L, R110W and I298fsX307, also localized to the nucleus. However, the R39X GCMB mutant was distributed in both the nucleus and cytoplasm, similar to that observed with EGFP alone, thereby demonstrating that this nonsense GCMB mutant has disrupted nuclear localization. Images were captured under identical conditions. Scale bar = 10 μm.

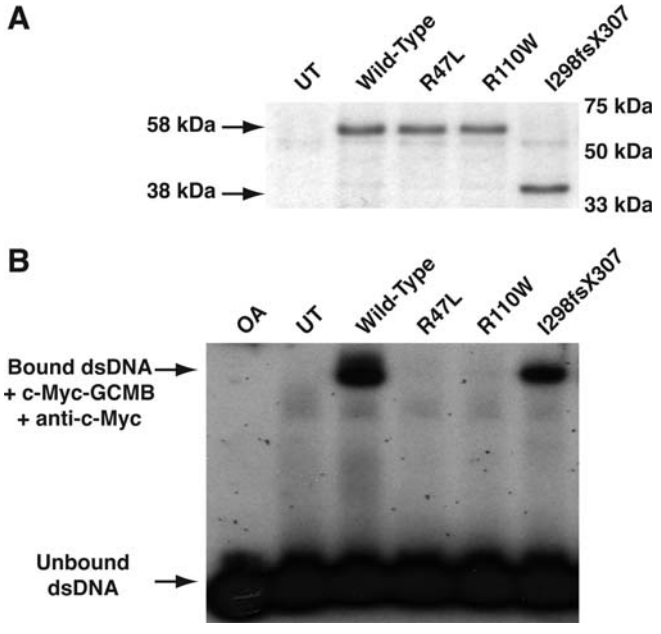

Figure 5. Analysis of DNA-binding properties of wild-type and GCMB mutants associated with AR-HPT. (**A**) Western blot analysis of cell lysates obtained from COS-7 cells transiently transfected with c-Myc-tagged GCMB wild-type or mutant constructs. Use of a c-Myc monoclonal antibody detected the expected 58 kDa GCMB wild-type and mutant, R47L and R110W, proteins. However, the GCMB frameshift deletion (I298fsX307) yielded the predicted truncated 38 kDa product (Table 2). An untransfected cell lysate (UT) was used as a control. (**B**) Electrophoretic mobility shift assay, EMSA. COS-7 cells were transfected with either the wild-type or mutant c-Myc-tagged GCMB constructs, and whole cell lysates were prepared for binding reactions, which used a (32)P-radiolabeled double-stranded (ds) oligonucleotide containing the GCM consensus DNA sequence (15,17,18) and an anti-c-Myc antibody (9E10). Control binding reactions using untransfected (UT) cell lysates and oligonucleotide alone (OA), i.e. without nuclear extract, were performed. Wild-type GCMB protein bound the dsDNA oligonucleotide, whereas the two GCMB missense mutants (R47L and R110W), which alter residues within the DBD (Fig. 1), did not bind the dsDNA oligo. However, the frameshift deletion (I298fsX307) GCMB mutant retained the ability to bind the GCM consensus DNA sequence.

I298fsX307, occurred within such repeat elements, and the underlying mechanisms causing these remain to be elucidated.

Our functional studies provide interesting insights into the structural–functional relationships of the GCM domains. Thus, the mutations that disrupt the GCM DBD, lead to a loss of DNA binding (Fig. 5), whereas the C-terminal truncation does not lead to a loss of DNA binding, but instead reduces the transactivational ability of the protein (Fig. 7). The two missense mutations, R47L and R110W (Fig. 1 and Table 2), which result in alterations of evolutionarily conserved basic residues within the DBD of the GCM family members, are predicted to disrupt the tertiary structure of the DBD (Fig. 6). This in turn is predicted to result in a loss of DNA binding (Fig. 5) and hence a likely reduction in the transcription of target genes. In contrast to the GCM DBD missense mutants, the frameshift-deletion mutant, I298fsX307, retains DNA-binding ability (Fig. 5), but has a reduced transactivation potential due to lack of the C-terminal TAD2 (amino acids 428–506) (Figs 1 and 7). This is consistent with previous studies that have shown TAD2 to be important for the transactivation potential of mouse Gcm2 (33). Interestingly, the transactivational ability of the truncated I298fsX307 mutant, which still retains TAD1, is comparable to that observed for the two missense mutants (R47L and R110W) that fail to bind DNA, suggesting that TAD2 is the major determining factor of GCMB transactivation potential. In addition, the I298fsX307 mutation only resulted in AR-HPT in homozygous individuals, but not in heterozygous individuals (Fig. 2), demonstrating the recessive nature of this mutation. However, when the heterozygous state

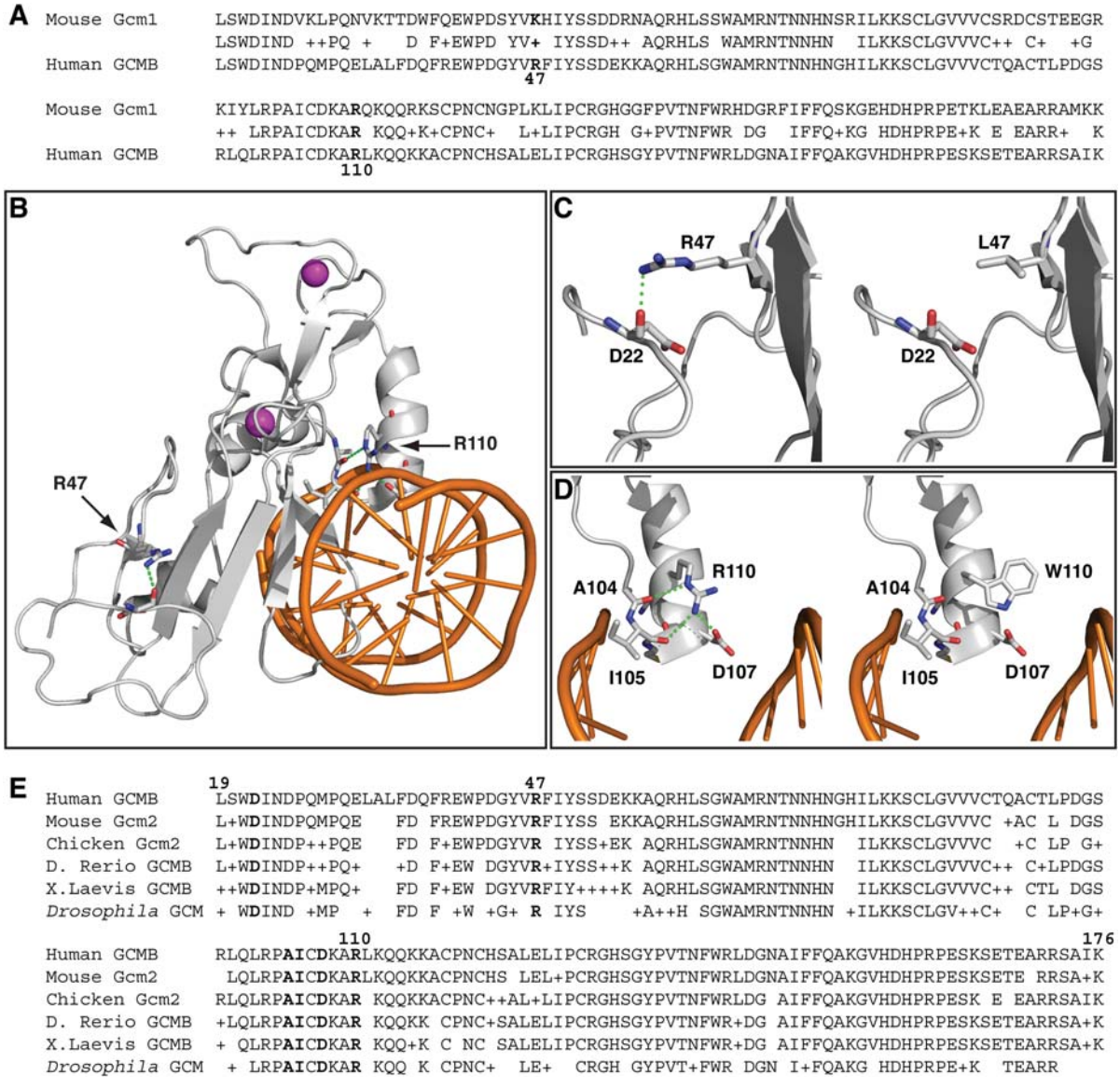

Figure 6. Sequence alignment and three-dimensional modelling of the human GCMB DBD. The mammalian GCM proteins, GCMA and GCMB in man and Gcm1 and Gcm2 in mouse, have a conserved GCM DBD (Fig. 1). (**A**) Protein sequence alignment of the DBD of mouse Gcm1 (residues 14–171) and human GCMB (residues 19–176) using BLAST 2 sequences (39) revealed a 68% identity between the two domains. Amino acid residues shared between these DBDs are shown, similar residues are depicted with a plus sign, and non-conserved residues are indicated by a gap. This level of homology allows a reliable model of the GCMB DBD in complex with DNA to be determined by comparative modelling, based on the previously published Gcm1 DBD-DNA crystal structure (PDB ID: 1ODH_A) (25). The locations of the GCMB residues, R47 and R110, are numbered and shown in bold. (**B**) The model of the GCMB DBD (residues 19–176) in complex with DNA (5′-CGATGCGGGTGCA-3′) is shown with the protein shown in grey, DNA double-helix coloured orange and two coordinated Zn^{2+} atoms as magenta spheres. The residues D22, R47, A104, I105, D107 and R110 are shown in stick presentation coloured by element (carbon, grey; oxygen, red; nitrogen, blue) and polar side-chain contacts made by R47 and R110 are shown as dotted green lines. (**C**) Expanded view of the structural effect of the R47L GCMB mutant causing AR-HPT. Models of the wild-type R47, and mutant L47 proteins are shown on the left and right, respectively, with important residues shown in stick presentation coloured by element. In the wild-type model (left), the side-chain hydrogen bond formed between the nitrogen of R47 and the oxygen of D22 is depicted as a dotted green line. In the mutant model (right), a hydrogen bond cannot form between L47 and D22. This hydrogen bond is very near the N-terminal of the protein and is likely to be required for the correct folding or stabilization of the mature protein. Thus, loss of this polar side-chain interaction in the R47L mutant is likely to lead to mis-folding or destabilization of the GCMB protein. (**D**) Expanded view of the structural effect of the R110W GCMB mutant causing AR-HPT. Models of the wild-type R110, and mutant W110 proteins are shown on the left and right, respectively. In the wild-type model (left), three side-chain hydrogen bonds (dotted green lines) are predicted to form between R110 and the highly conserved residues A104, I105 and D107. In the mutant model (right), these hydrogen bonds cannot form between W110 and these residues. The hydrogen bonds, present in the wild-type protein, formed by R110, located in helix 2, are likely required for the stabilization of the strand-bend-helix structure that fits into the DNA groove. In addition to loss of these potentially stabilizing polar contacts in the mutant protein, it is also important to recognize that the aromatic side chain of the mutant W110 residue has a larger van der Waals volume than the wild-type R110 residue, and therefore this could also lead to destabilization of the strand-bend-helix structure. (**E**) These residues (D22, A104, I105 and D107) that are important for the functional effects of the R47L and R110W mutations are highly evolutionarily conserved and shown bold on protein sequence alignment of the DBD of human GCMB (residues 19–176), mouse Gcm2, chicken Gcm2, *D.* Rerio GCMB, *X.* Laevis GCMB, and *Drosophila* GCM, using BLAST 2 sequences (39). Amino acid residues shared with Human GCMB DBD are shown, similar residues are depicted with a plus sign, and non-conserved residues are indicated by a gap.

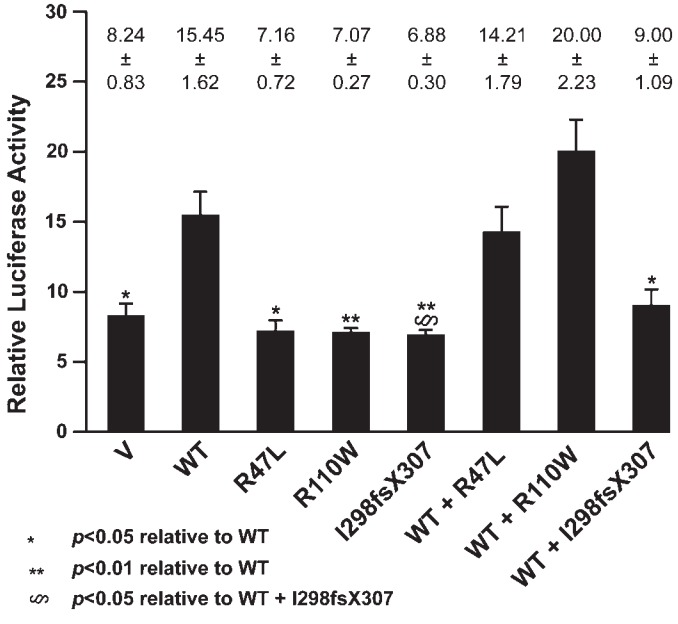

Figure 7. Luciferase reporter assay of wild-type and mutant GCMBs associated with AR-HPT. Wild-type and mutant GCMB constructs were co-transfected with the pGL3-CaSR luciferase reporter vector (pGL3-CaSR luc) containing a GCMB binding site and a plasmid encoding Renilla luciferase (pRL-null Vector) into DF-1 cells. Cells were harvested 48 h after transfection and assayed for luciferase activity. Three separate experiments were performed in triplicate, and the data are represented as mean firefly: renilla ratio ± SEM of all experiments. Wild-type (WT) GCMB expression resulted in 2-fold increase in relative luciferase activity when compared with transfection with the empty pCMV-Myc vector (V). Expression of the GCMB mutants (R47L, R110W or I298fsX307) alone failed to increase the relative luciferase activity above that observed with the empty vector. However, co-transfection of the wild-type GCMB with the GCMB mutants R47L and R110W (WT + R47L, WT + R110W) restored luciferase activity, whereas co-transfection with the I298fsX307 GCMB mutant (WT + I298fsX307) failed to restore the full luciferase activity.

was mimicked in the *in vitro* luciferase reporter assay (I298fsX307 + wild-type), the transactivation potential was only slightly increased compared with I298fsX307 alone, whereas the missense mutants co-transfected with wild-type recovered a transactivation potential comparable with wild-type. This could suggest that the I298fsX307 mutant is acting in a partial dominant-negative fashion, or that the critical threshold dosage requirement for GCMB is very low, and that only a complete absence of functional GCMB protein would result in AR-HPT. This would be consistent with the findings from the Gcm2 mouse knockout model in which only $Gcm2^{-/-}$ mice developed hypocalcaemia and hypoparathyroidism (22). This would suggest that GCMB function may not depend on gradations in the dosage of the transcription factor, as reported for other transcription factors (34,35), but may instead depend on an 'on-off' binary mechanism.

Our studies demonstrate the importance of GCMB in the aetiology of autosomal recessive-isolated hypoparathyroidism, particularly within families from the Indian subcontinent where *GCMB* mutations may account for up to 80% of cases, and highlight that *GCMB* gene mutational analysis be undertaken even when there is no evidence of parental consanguinity. Finally, ~33% of probands with AR-HPT in our study did not have *GCMB* coding region or splice site mutations, even though they were clinically indistinguishable from those who had GCMB mutations (Table 1). This reflects the genetic heterogeneity of AR-HPT, which may also be caused by *PTH* mutations (5,6), or mutation of as-yet-unidentified genes. In conclusion, our results expand the spectrum of AR-HPT associated *GCMB* mutations and increase our understanding of mechanisms by which *GCMB* mutations cause this developmental disorder.

MATERIALS AND METHODS

Patients

Eighteen patients from 12 families with AR-HPT were ascertained. Ten of these families originated from the North-West region of the Indian Subcontinent and two families, in whom GCMB mutations were not identified, originated from the Middle East and Somalia in the Horn of Africa (Table 1). All of the affected individuals were hypocalcaemic with serum calcium ranging from 0.90 to 2.02 mmol/l, and this was associated with tetany or seizures in 15 patients (Table 1).

DNA sequence analysis of the *GCMB* gene

Venous blood was obtained after informed consent, as approved by the local ethical committee (MREC/02/2/93), and used to extract leukocyte DNA (10). Eight pairs of *GCMB*-specific primers (details available on request) were used for the PCR amplification of the five coding exons and adjoining splice junctions (Fig. 1) utilizing 150 ng of genomic DNA. The DNA sequences of both strands were determined by *Taq* polymerase cycle sequencing and resolved on a semi-automated detection system (ABI 377 sequencer; PE Applied Biosystems, Foster City, CA, USA) (10). DNA sequence abnormalities were confirmed by restriction endonuclease analysis, using methods previously described (10).

Microsatellite polymorphic loci

The genotypes at the microsatellite polymorphic loci *D6S470*, *D6S1721*, *D6S1653* from chromosome 6p23-24 (8) were determined using a 5′ fluorescently labelled forward primer and an unlabelled reverse primer, as previously described (36).

GCMB constructs

A wild-type GCMB construct was prepared in pGEM-T (Promega) and used as a template for the generation of mutant GCMB constructs by use of site-directed mutagenesis (Quikchange, Stratagene, CA, USA) (37). The DNA sequences of all constructs were verified by *Taq* polymerase cycle sequencing and resolved on a semi-automated detection system (ABI 377 sequencer; PE Applied Biosystems, Foster City, CA, USA), as previously described (10). The wild-type and mutant GCMB constructs were subcloned in-frame into the mammalian expression vectors pEGFP-C3 and pCMV-Myc (BD Biosciences Clontech, CA, USA), to yield GCMB tagged at the N-terminus with EGFP or c-Myc, respectively (10,38).

Nuclear localization studies using enhanced green fluorescent protein–GCMB fusion constructs

COS-7 cells were cultured on glass coverslips to 50–60% confluency, and transiently transfected with 0.4 μg DNA of the appropriate expression construct using FuGENE 6 (Roche, Basel, Switzerland). Twenty-four hours post-transfection, the cells were washed with phosphate buffered saline (PBS), fixed in 4% paraformaldehyde, permeabilized using Triton X-100 (0.5% v/v) containing RNaseA (100 μg/ml), stained with propidium iodide (3 μg/ml) (Sigma, MO, USA) and mounted with Vectashield (Vector Laboratories, CA, USA) (38). The subcellular localizations of the fusion proteins were visualized using a Nikon Eclipse fluorescence microscope and NIS-elements BR 2.30 imaging software (27). Images were recorded under identical conditions.

Electrophoretic mobility shift assays (EMSAs)

COS-7 cells, which do not endogenously express *GCMB*, were transfected with either a wild-type or mutant c-Myc-tagged GCMB construct. Forty-eight hours post-transfection, the cells were harvested, and total cell extracts were prepared, as previously described (18). Western blot analysis using 9E10 monoclonal antibody (Santa Cruz Biotechnology, Inc., Santa Cruz, CA, USA) against c-Myc confirmed the presence of GCMB-tagged protein in the extracts. For super-shift EMSAs, extracts were incubated for 10 min on ice, 1 μl 9E10 antibody added and incubated on ice for a further 10 min before addition of 0.5 ng of a (32)P-labelled double-stranded oligonucleotide containing the GCM consensus, as previously described (18). After a 20 min incubation on ice, the binding reactions were loaded onto native-polyacrylamide gels and electrophoresed in 0.5X TBE at 200 V for 40 min. Gels were dried and exposed for autoradiography.

Computer modelling of GCMB DNA-binding domain structure

The evolutionary conservation of human GCMB residues and their homologies to mouse Gcm1, and other vertebrate and invertebrate GcmB factors were assessed using the online *Basic Local Alignment Search Tool* (BLAST) available at the NCBI website (http://blast.ncbi.nlm.nih.gov/Blast.cgi) (39). The three-dimensional crystal structure of the murine Gcm1 GCM DNA-binding domain in complex with DNA has been reported (25), and because the DNA-binding domains of mouse Gcm1 and human GCMB are 68% identical (82% similar), we modelled the position of the GCMB mutants R47L and R110W, on this framework. The mouse Gcm1 GCM domain-DNA complex three-dimensional structure is archived in the Protein Data Bank (PDB) at the European Bioinformatics Institute (EBI) with the PDB ID: 1ODH_A (http://www.ebi.ac.uk/pdbe/), and was visualized using the MacPyMOL program (DeLano Scientific LLC).

Generation of luciferase reporter constructs and assays

To test the transcriptional activity of GCMB mutant proteins, a CaSR-promoter luciferase reporter construct, containing an endogenous GCMB DNA motif (13), was generated by PCR amplification of the promoter region and exon 1A (40) from genomic DNA using the forward primer *CaSR-pr-F* tagged with a *KpnI* restriction site (5′-ggtaccatgcccaggtgtaatccgacc) and reverse primer *CaSR-pr-R* tagged with *XmaI* restriction site (5′-cccgggccaaactcttactcattctg). This PCR product was subcloned into pGEM-T (pGEM-T-promoter construct). An expressed sequence tag (EST) clone was obtained from I.M.A.G.E. consortium (IMAGE: 5925-107) and was used in PCR amplification of CaSR cDNA containing the partial exon 1A (overlapping with promoter sequence cloned into pGEM-T) and exon 2 using forward primer *CaSR-Im-F* (5′-aaggagggagctgtttgccagc), and reverse primer *CaSR-Im-R* tagged with *XmaI* restriction site (5′-cccgggttctgccgtctctcca gggca). This PCR product was subcloned into pGEM-T, digested with *PshAI* and *XmaI*, and ligated into pGEM-T-promoter construct digested with the same enzymes. The fused promoter region, exon 1A and exon 2, were digested from pGEM-T with *KpnI* and *XmaI* and cloned upstream of the luciferase gene into pGL3 basic vector (Promega) digested with the same enzymes. The DNA sequences of both strands of the pGL3-CaSR lucifera se reporter construct were verified by *Taq* polymerase cycle sequencing and resolved on a semi-automated detection system (ABI 377 sequencer; PE Applied Biosystems, Foster City, CA, USA) (10).

DF-1 cells were transiently transfected in 24-well plates with a total of 400 ng of plasmid DNA per well using FuGENE 6 transfection reagent as follows: 100 ng/well of pGL3-CaSR luciferase reporter plasmid containing a GCMB binding site in its promoter; 0.5 ng/well of plasmid encoding Renilla luciferase (pRL-null Vector; Promega, Madison, WI, USA) to allow normalization of the data; and a total of 300 ng of plasmid encoding wild-type or mutant GCMB and, when appropriate, empty vector pCMV-Myc to keep the amount of transfected plasmid DNA constant. Cells were harvested 48 h after transfection and assayed for luciferase activity using the Dual Luciferase Reporter Assay (Promega, Madison, WI, USA). Three experiments were carried out in triplicate, and the data are represented as mean firefly: renilla ratio ± SEM of all experiments, as previously reported (27).

ACKNOWLEDGEMENTS

S.M.M. is a Medical Research Council PhD student.

Conflict of Interest statement. None declared.

FUNDING

This work was supported by the UK Medical Research Council (grant G9825289) (to M.R.B, S.M.M., I.V.G., M.A.N. and R.V.T.).

REFERENCES

1. Thakker, R.V. (2001) Genetic developments in hypoparathyroidism. *Lancet*, **357**, 974–976.

2. Thakker, R.V. (2004) Diseases associated with the extracellular calcium-sensing receptor. *Cell Calcium*, **35**, 275–282.
3. Thakker, R.V. and Juppner, H. (2006) Genetic disorders of calcium homeostasis caused by abnormal regulation of parathyroid hormone secretion or responsiveness. De Groot, L.J. and Jameson, J.L. (eds), *Endocrinology.*, 5th edn. Elsevier, pp. 1511–1531.
4. Marx, S.J. (2000) Hyperparathyroid and hypoparathyroid disorders. *N. Engl. J. Med.*, **343**, 1863–1875.
5. Parkinson, D.B. and Thakker, R.V. (1992) A donor splice site mutation in the parathyroid hormone gene is associated with autosomal recessive hypoparathyroidism. *Nat. Genet.*, **1**, 149–152.
6. Sunthornthepvarakul, T., Churesigaew, S. and Ngowngarmratana, S. (1999) A novel mutation of the signal peptide of the preproparathyroid hormone gene associated with autosomal recessive familial isolated hypoparathyroidism. *J. Clin. Endocrinol. Metab.*, **84**, 3792–3796.
7. Arnold, A., Horst, S.A., Gardella, T.J., Baba, H., Levine, M.A. and Kronenberg, H.M. (1990) Mutation of the signal peptide-encoding region of the preproparathyroid hormone gene in familial isolated hypoparathyroidism. *J. Clin. Invest.*, **86**, 1084–1087.
8. Ding, C., Buckingham, B. and Levine, M.A. (2001) Familial isolated hypoparathyroidism caused by a mutation in the gene for the transcription factor GCMB. *J. Clin. Invest.*, **108**, 1215–1220.
9. Bowl, M.R., Nesbit, M.A., Harding, B., Levy, E., Jefferson, A., Volpi, E., Rizzoti, K., Lovell-Badge, R., Schlessinger, D., Whyte, M.P. *et al.* (2005) An interstitial deletion-insertion involving chromosomes 2p25.3 and Xq27.1, near SOX3, causes X-linked recessive hypoparathyroidism. *J. Clin. Invest.*, **115**, 2822–2831.
10. Nesbit, M.A., Bowl, M.R., Harding, B., Ali, A., Ayala, A., Crowe, C., Dobbie, A., Hampson, G., Holdaway, I., Levine, M.A. *et al.* (2004) Characterization of GATA3 mutations in the hypoparathyroidism, deafness, and renal dysplasia (HDR) syndrome. *J. Biol. Chem.*, **279**, 22624–22634.
11. Thomee, C., Schubert, S.W., Parma, J., Le, P.Q., Hashemolhosseini, S., Wegner, M. and Abramowicz, M.J. (2005) GCMB mutation in familial isolated hypoparathyroidism with residual secretion of parathyroid hormone. *J. Clin. Endocrinol. Metab.*, **90**, 2487–2492.
12. Baumber, L., Tufarelli, C., Patel, S., King, P., Johnson, C.A., Maher, E.R. and Trembath, R.C. (2005) Identification of a novel mutation disrupting the DNA binding activity of GCM2 in autosomal recessive familial isolated hypoparathyroidism. *J. Med. Genet.*, **42**, 443–448.
13. Canaff, L., Zhou, X., Mosesova, I., Cole, D.E. and Hendy, G.N. (2009) Glial cells missing-2 (GCM2) transactivates the calcium-sensing receptor gene: effect of a dominant-negative GCM2 mutant associated with autosomal dominant hypoparathyroidism. *Hum. Mutat.*, **30**, 85–92.
14. Mannstadt, M., Bertrand, G., Muresan, M., Weryha, G., Leheup, B., Pulusani, S.R., Grandchamp, B., Juppner, H. and Silve, C. (2008) Dominant-negative GCMB mutations cause an autosomal dominant form of hypoparathyroidism. *J. Clin. Endocrinol. Metab.*, **93**, 3568–3576.
15. Akiyama, Y., Hosoya, T., Poole, A.M. and Hotta, Y. (1996) The gcm-motif: a novel DNA-binding motif conserved in Drosophila and mammals. *Proc. Natl Acad. Sci. USA*, **93**, 14912–14916.
16. Cohen, S.X., Moulin, M., Schilling, O., Meyer-Klaucke, W., Schreiber, J., Wegner, M. and Muller, C.W. (2002) The GCM domain is a Zn-coordinating DNA-binding domain. *FEBS Lett.*, **528**, 95–100.
17. Schreiber, J., Sock, E. and Wegner, M. (1997) The regulator of early gliogenesis glial cells missing is a transcription factor with a novel type of DNA-binding domain. *Proc. Natl Acad. Sci. USA*, **94**, 4739–4744.
18. Schreiber, J., Enderich, J. and Wegner, M. (1998) Structural requirements for DNA binding of GCM proteins. *Nucleic Acids Res.*, **26**, 2337–2343.
19. Basyuk, E., Cross, J.C., Corbin, J., Nakayama, H., Hunter, P., Nait-Oumesmar, B. and Lazzarini, R.A. (1999) Murine Gcm1 gene is expressed in a subset of placental trophoblast cells. *Dev. Dyn.*, **214**, 303–311.
20. Hashemolhosseini, S., Hadjihannas, M., Stolt, C.C., Haas, C.S., Amann, K. and Wegner, M. (2002) Restricted expression of mouse GCMa/Gcm1 in kidney and thymus. *Mech. Dev.*, **118**, 175–178.
21. Kim, J., Jones, B.W., Zock, C., Chen, Z., Wang, H., Goodman, C.S. and Anderson, D.J. (1998) Isolation and characterization of mammalian homologs of the Drosophila gene glial cells missing. *Proc. Natl Acad. Sci. USA*, **95**, 12364–12369.
22. Gunther, T., Chen, Z.F., Kim, J., Priemel, M., Rueger, J.M., Amling, M., Moseley, J.M., Martin, T.J., Anderson, D.J. and Karsenty, G. (2000) Genetic ablation of parathyroid glands reveals another source of parathyroid hormone. *Nature*, **406**, 199–203.
23. Maret, A., Ding, C., Kornfield, S.L. and Levine, M.A. (2008) Analysis of the GCM2 gene in isolated hypoparathyroidism: a molecular and biochemical study. *J. Clin. Endocrinol. Metab.*, **93**, 1426–1432.
24. Hashemolhosseini, S. and Wegner, M. (2004) Impacts of a new transcription factor family: mammalian GCM proteins in health and disease. *J. Cell Biol.*, **166**, 765–768.
25. Cohen, S.X., Moulin, M., Hashemolhosseini, S., Kilian, K., Wegner, M. and Muller, C.W. (2003) Structure of the GCM domain-DNA complex: a DNA-binding domain with a novel fold and mode of target site recognition. *EMBO J.*, **22**, 1835–1845.
26. Sticht, H. and Hashemolhosseini, S. (2006) A common structural mechanism underlying GCMB mutations that cause hypoparathyroidism. *Med. Hypotheses*, **67**, 482–487.
27. Gaynor, K.U., Grigorieva, I.V., Nesbit, M.A., Cranston, T., Gomes, T., Gortner, L. and Thakker, R.V. (2009) A missense GATA3 mutation, Thr272Ile, causes the hypoparathyroidism, deafness, and renal Dysplasia syndrome. *J. Clin. Endocrinol. Metab.*, **94**, 3897–3904.
28. Benzer, S. (1961) On the topography of the genetic fine structure. *Proc. Natl Acad. Sci. USA*, **47**, 403–415.
29. Ripley, L.S. (1982) Model for the participation of quasi-palindromic DNA sequences in frameshift mutation. *Proc. Natl Acad. Sci. USA*, **79**, 4128–4132.
30. Bebenek, K. and Kunkel, T.A. (2000) Streisinger revisited: DNA synthesis errors mediated by substrate misalignments. *Cold Spring Harb. Symp. Quant. Biol.*, **65**, 81–91.
31. Kunkel, T.A. (1985) The mutational specificity of DNA polymerase-beta during in vitro DNA synthesis. Production of frameshift, base substitution, and deletion mutations. *J. Biol. Chem.*, **260**, 5787–5796.
32. Kunkel, T.A. and Soni, A. (1988) Mutagenesis by transient misalignment. *J. Biol. Chem.*, **263**, 14784–14789.
33. Tuerk, E.E., Schreiber, J. and Wegner, M. (2000) Protein stability and domain topology determine the transcriptional activity of the mammalian glial cells missing homolog, GCMb. *J. Biol. Chem.*, **275**, 4774–4782.
34. Pan, X., Ohneda, O., Ohneda, K., Lindeboom, F., Iwata, F., Shimizu, R., Nagano, M., Suwabe, N., Philipsen, S., Lim, K.C. *et al.* (2005) Graded levels of GATA-1 expression modulate survival, proliferation, and differentiation of erythroid progenitors. *J. Biol. Chem.*, **280**, 22385–22394.
35. Rosenbauer, F., Koschmieder, S., Steidl, U. and Tenen, D.G. (2005) Effect of transcription-factor concentrations on leukemic stem cells. *Blood*, **106**, 1519–1524.
36. Stacey, J.M., Turner, J.J., Harding, B., Nesbit, M.A., Kotanko, P., Lhotta, K., Puig, J.G., Torres, R.J. and Thakker, R.V. (2003) Genetic mapping studies of familial juvenile hyperuricemic nephropathy on chromosome 16p11-p13. *J. Clin. Endocrinol. Metab.*, **88**, 464–470.
37. Kennedy, A.M., Inada, M., Krane, S.M., Christie, P.T., Harding, B., Lopez-Otin, C., Sanchez, L.M., Pannett, A.A., Dearlove, A., Hartley, C. *et al.* (2005) MMP13 mutation causes spondyloepimetaphyseal dysplasia, Missouri type (SEMD(MO). *J. Clin. Invest.*, **115**, 2832–2842.
38. Bradley, K.J., Bowl, M.R., Williams, S.E., Ahmad, B.N., Partridge, C.J., Patmanidi, A.L., Kennedy, A.M., Loh, N.Y. and Thakker, R.V. (2007) Parafibromin is a nuclear protein with a functional monopartite nuclear localization signal. *Oncogene*, **26**, 1213–1221.
39. Tatusova, T.A. and Madden, T.L. (1999) BLAST 2 Sequences, a new tool for comparing protein and nucleotide sequences. *FEMS Microbiol. Lett.*, **174**, 247–250.
40. Canaff, L. and Hendy, G.N. (2002) Human calcium-sensing receptor gene. Vitamin D response elements in promoters P1 and P2 confer transcriptional responsiveness to 1,25-dihydroxyvitamin D. *J. Biol. Chem.*, **277**, 30337–30350.